Interval Fields for Geotechnical Engineering Uncertainty Analysis under Limited Data

Chengxin Feng[1], Matteo Broggi[2], Yue Hu[3], Matthias G.R. Faes[4], and Michael Beer[5]

[1]Ph.D. Candidate, Institute for Risk and Reliability, Leibniz Univ. Hannover, Hannover 30167, Germany (corresponding author). Email: feng.chengxin@irz.uni-hannover.de

[2]Deputy Institute Director, Institute for Risk and Reliability, Leibniz Univ. Hannover, Hannover 30167, Germany.

[3]Postdoctoral Research Associate, Institute for Risk and Reliability, Leibniz Univ. Hannover, Hannover 30167, Germany.

[4]Professor and Chair for Reliability Engineering, Dept. of Mechanical Engineering, TU Dortmund Univ., Leonhard-Euler-Strasse 5, Dortmund 44227, Germany.

[5]Professor and Institute Director, Institute for Risk and Reliability, Leibniz Univ. Hannover, Callinstr. 34, Hannover 30167, Germany; Department of Civil and Environmental Engineering, Univ. of Liverpool, Liverpool L69 7ZF, UK; International Joint Research Center for Resilient Infrastructure & International Joint Research Center for Engineering Reliability and Stochastic Mechanics, Tongji Univ., Shanghai 200092, China.

ABSTRACT

Spatial uncertainty is a critical challenge in many engineering fields. To date, the probabilistic methods have been applied to describe the uncertainty of engineering parameters with considerable achievements. However, they rely heavily on the availability of large quantities of informative data, while in practice, acquiring enough informative data is impossible. This paper proposes an interval field-based framework to analyze the influence of parameter uncertainty on their safety performance under sparse test data, in which the locations of test values are taken into account. It

also considers uncertainties in stratigraphy and spatial properties in the geotechnical engineering case, allowing the research framework to utilize more available test information compared to previous studies. First, the interval field samples based on B-spline basis functions are generated, allowing for flexibility in accounting for realistic situations and integrating measured data from in situ exploration. Then, the finite element strength reduction method is used to estimate the safety factor (f_s) of geotechnical engineering. Subsequently, a Bayesian global optimization is used to efficiently evaluate the upper and lower bounds of the f_s interval. Finally, three geotechnical engineering cases are presented to illustrate the validity of the proposed framework. This framework provides new insights into engineering uncertainty analysis even with sparse data, highlighting its potential for practical applications in geotechnical engineering projects.

INTRODUCTION

Engineering decision making in geotechnical projects often is complicated because of the uncertainty stemming from the inherent variability of materials, processes, and environmental conditions (Der Kiureghian and Ditlevsen 2009). In structural engineering, where man-made materials exhibit relative homogeneity, this variability is often quantified using random variables (Ellingwood et al. 2024). It allows for probabilistic analysis of structural behavior, providing valuable insights into potential performance (Phoon 2023). However, natural materials such as soils and rocks present a unique challenge: spatial uncertainty. Unlike their man-made counterparts, these materials exhibit significant spatial variability in their properties, meaning their characteristics can vary considerably across a given area (Phoon and Kulhawy 1999). Disregarding this spatial uncertainty can have significant ramifications for project safety and performance. For example, in geotechnical engineering, neglecting the spatial variation in soil properties can lead to underestimation of foundation settlements, slope instability, and embankment dam failure (Xiao et al. 2017; Guo et al. 2019; Wang et al. 2020; Feng et al. 2024). Similarly, hydrological models that fail to account for the spatial distribution of rainfall and infiltration rates can result in inaccurate flood predictions (McMillan et al. 2011). Therefore, the consideration of spatial uncertainty is paramount for ensuring the safety and reliability of infrastructure projects.

For several decades, scholars have developed a series of mathematical models for spatial uncertainty analysis, with the random field method standing out as one of the most widely employed techniques (Chwała et al. 2022; Jiang et al. 2022; Wang et al. 2023). Leveraging concepts from well-established probability theory, random fields serve as a robust tool for characterizing spatial uncertainty of material parameters (Phoon and Ching 2018). In the domain of geotechnical engineering, random fields find primarily application in capturing uncertainties pertaining to boundary conditions, geological features, and parameter properties (Juang et al. 2019). To construct such random fields to represent spatial uncertainties, techniques such as the Karhunen-Loève expansion, orthogonal series expansion, expansion optimal linear estimation, and perturbation method have been developed (Sudret and Der Kiureghian 2000; Zhang et al. 2022). However, the complicated nature of different engineering uncertainties often necessitates adaptations to the traditional approach. For example, in the field of geotechnical engineering, the uncertainty of the stratigraphic boundary will affect the geologic model (Juang et al. 2019). This type of uncertainty provides challenges for traditional random field models because statistical coefficients for a limited number of borehole data may significantly affect simulated stratigraphic samples (Liu and Wang 2022). In practice, when dealing with stratigraphic uncertainty, specialized simulation methods are employed. These approaches include coupled Markov chains, stochastic Markov random fields, and improved conditional random field techniques (Gong et al. 2021; Zhao et al. 2021; Yan et al. 2023).

There have been significant advances in the random field method, but challenges remain, especially when dealing with limited data. In the process of modeling geotechnical uncertainty with random field expansion, a critical step involves the determination of the statistical parameters to describe the spatial uncertainty. These parameters encompass the mean and variance in the assumed lognormal distribution, as well as the autocorrelation function, which might be governed by a correlation length in the case of isotropic random fields. Typically, these parameters are derived using methods like moments or maximum likelihood estimation, both of which often necessitate substantial volumes of experimental data (Cami et al. 2020). Also, Bayesian model updating techniques have been proposed in a different context (Uribe et al. 2020). However, the limited

information that can be obtained from engineering site investigations tends to constrain efforts due to time and especially cost constraints. Consequently, due to these practical limitations, the modeling of geological stratification and parameter uncertainty can only be performed with sparse data, which may cause the uncertainty in the estimated parameters to be significant (Montoya-Noguera et al. 2019; Beer et al. 2013). In addition, making an assumption of probability distributions based on expert knowledge is often required. Recently, the Bayesian compressive sampling method has been proposed and achievements have been made (Zhao et al. 2018; Wang et al. 2018). The Bayesian compressive sampling developments are generally fit for a specific distribution type of spatial variability.

As an alternative to the random field model, interval fields have been proposed for representing spatial uncertainty and have been successfully applied in engineering (Moens et al. 2011; Feng et al. 2022). In essence, the research on interval fields consists of three main steps, and current research focuses on these: (1) interval field parameter identification and quantification, (2) interval field generation, and (3) the propagation of interval fields (Faes and Moens 2020b). To identify and quantify interval field parameters, Faes and Moens (2017a) introduced a method to identify spatial uncertainty based on measurement data. Presently, techniques for constructing interval fields primarily involve the inverse distance weighted interpolation method (Faes and Moens 2017b; van Mierlo et al. 2021; Callens et al. 2021), Karhunen-Loève-like decomposition method (Sofi 2015), B-spline method (Hu et al. 2022) and techniques based on convex set representations (Jiang et al. 2011). Particularly, the B-spline basis function-based interval field method shows a lot of promise due to the flexibility of its B-spline formulation of the basis functions to flexibly model curves and surfaces. Its primary benefit lies in enabling local control of curves or surfaces, proving particularly valuable for fitting parameters obtained from test points. Finally, concerning propagation, many methods have been developed in recent years, among which optimization methods are widely used due to their efficiency (Faes and Moens 2020b). In particular, the Bayesian global optimization method has developed rapidly among many optimization methods due to its high efficiency and accuracy and has been applied in the uncertainty propagation of interval fields (Dang et al. 2022).

In previous work, the effectiveness of interval fields in engineering uncertainty analysis has been investigated (Feng et al. 2022). However, it has not considered the uncertainty analysis involving complex models with multiple uncertainties and sparse site test data and its advantages with related methods. In light of the limitations in current uncertainty quantification methods for complex and data-scarce engineering problems, this paper proposes a novel framework that leverages the interval field method. The proposed framework demonstrates comprehensive capabilities in quantifying uncertainties, such as stratigraphic and spatial properties in geotechnical engineering. Furthermore, it integrates in-situ testing data into the interval field description, thereby significantly reducing local epistemic uncertainty stemming from data scarcity. First, B-spline basis functions are adopted to generate interval fields because of their suitability in capturing complex behaviors. The localized data of the interval field is realized by controlling the interval variable at that position. Additionally, dependencies in both horizontal and vertical directions are used to represent the spatial uncertainty. Subsequently, the factor of safety (f_s) for geotechnical engineering is computed through the finite element strength reduction method. The interval boundaries of f_s are ultimately determined using the Bayesian global optimization method because of its capability to handle complex and nonlinear systems efficiently. The effectiveness of the framework proposed in this paper is demonstrated through the analysis of three real-world engineering cases. This advancement not only proposed a method for sparse data but also provided powerful tools for engineers dealing with complex and local data scenarios.

The paper follows the structure outlined below. In Section 2, the approach for generating interval fields through B-spline basis functions is detailed. Section 3 describes the procedure for analyzing engineering with uncertainties using the proposed interval field framework. Three actual engineering cases are demonstrated to illustrate the effectiveness of the method in Section 4. Finally, Section 5 presents the conclusions drawn from this study.

INTERVAL FIELDS BASED ON B-SPLINE BASIS FUNCTIONS

This section presents a general approach to generate interval field models based on B-spline basis functions, as introduced in (Hu et al. 2022). The section is constructed as follows: First, the

interval field and its explicit formulation are introduced. Subsequently, a detailed explanation of the method for generating interval fields based on B-spline basis functions is described in detail. Finally, the interval field method considering locally determined values is introduced.

Interval field

Interval fields are used to model spatial uncertainty in the presence of sparse data availability, which serves as the interval counterpart of the random field (Faes and Moens 2020b). This approach non-probabilistically characterizes spatial uncertainty in parameters through the establishment of upper and lower bounds. The methods for generating interval fields can be mainly categorized into explicit expansion methods and dependency function-based methods. In this paper specifically, we adopt the recently introduced B-spline basis functions to generate interval fields given their flexibility.

The general definition of the interval field can be expressed as

$$\psi^{\mathrm{I}}(\mathbf{x}) = \sum_{i=1}^{n} \omega_i(\mathbf{x}) \xi_i^{\mathrm{I}}, \tag{1}$$

where $\mathbf{x}$ are vector of control points, n is number of basis functions, $\psi^{\mathrm{I}}(\mathbf{x})$ represents the expression of the interval field, $\omega_i(\mathbf{x})$ denote the basis functions, and $\xi_i^{\mathrm{I}}, i = 1, \ldots, n$ are the n interval variables corresponding to the control points (Faes and Moens 2020a). Based on this formula, it becomes possible to generate interval fields involving spatial uncertainty. The significance of basis functions within this context cannot be overstated, as they must adequately capture the spatial nature of uncertainty in real-world engineering scenarios, and articulate it through a mathematical formulation.

As a small sidenote, we want to point out that by no means we imply that interval fields are always more *accurate* than random fields when less data are available. Their main feature is however that they allow for a fully objective investigation based on the knowledge that is available. In some cases, the results obtained from interval fields might be too uninformative for further analysis, indicating a need for additional data collection. Nonetheless, this decision would be made in this

case based on solid, objective analysis, which is provided by the interval framework.

B-spline basis function-based interval field

The method of generating interval fields with the B-spline basis functions is described in this subsection. This is based on the published work of Hu et al. (2022).

As explained in the previous section, the interval field can be generated according to Eq. 1. In this equation, especially the basis functions are of importance since the capture the spatial structure of the uncertainty. In this paper, the B-spline basis functions based on recursive formulas are used (Cox 1972; Piegl and Tiller 1996). To be specific, the forms of the B-spline basis functions are related to their degree, and the lower degree basis functions are needed when generating higher degree basis functions. When the degree of the B-spline basis function is 0, it can be expressed as

$$b_{i,0}(x) = \begin{cases} 1 & t_i \leqslant x < t_{i+1} \\ 0 & \text{otherwise} \end{cases}, \tag{2}$$

where $b_{i,0}(x)$ is i-th basis function, and t_i is i-th knot. For a B-spline basis function with a degree greater than one, the k-th B-spline basis function can be formulated as

$$b_{i,k}(x) = \frac{x - t_i}{t_{i+k} - t_i} b_{i,k-1}(x) + \frac{t_{i+k+1} - x}{t_{i+k+1} - t_{i+1}} b_{i+1,k-1}(x), \tag{3}$$

where k denotes the degree of the B-spline basis function. The computation of B-spline basis functions with higher degrees can be performed using this recursive formula. The B-spline basis function also needs to satisfy basic properties such as the partition of unity, which can be expressed as

$$\sum_{i=1}^{n} b_{i,k}(x) = 1, t_{k+1} \leqslant x \leqslant t_n, \tag{4}$$

where n is the number of the basis function. As described previously, the generation of an interval field requires a combination of the B-spline basis function and the interval parameters, which include the interval's center, radius, and dependence length. After the required parameters for the

interval field are determined in the domain, the visual representation of the interval field formulation can be achieved through the B-spline basis function-based interval field method, as follows:

$$\psi^{\mathrm{I}}(x) = c^I + r^I \sum_{i=1}^{N} b_{i,k}(x)\xi_i^{\mathrm{I}}, t_{k+1} \leqslant x \leqslant t_n, \tag{5}$$

where $\psi^{\mathrm{I}}(x)$ is interval field, c^I is the center value of the interval field, r^I is the radius of the interval field, and ξ_i^{I} are unitary interval variables. In this equation, the knot vectors control the spatial dependence of the points in the interval field, which is adjusted by the dependence length. The dependence length, which signifies the range over which the interval field exerts influence, is denoted as

$$r_d = (k+1)\Delta t/2, \tag{6}$$

where Δt is the distance between the knot vectors.

After determining the interval field parameters, the interval fields are calculated using Eqs. 2 to 6. The primary steps are outlined as follows. First, the process begins with the computation of knot vectors through the utilization of Eq. 6. Subsequently, B-spline basis functions are generated employing Eqs. 2 and 3, followed by the generation of the interval field using Eq. 5. To exemplify the result, we provide a concrete example showcasing 50 samples of a one-dimensional interval field, depicted in Fig. 1. In this example, the range of its interval field is 94, the center of the interval is one, the radius of the interval is 0.1, and the dependence length is 20.

One-dimensional interval fields have been generated based on the previous descriptions. However, there is still a difference between it and the two/three-dimensional interval fields that are required in geotechnical engineering, where the main difference is the form of the basis functions. It is important to note that we are assuming separable dependence structures in this analysis, which are not applicable to inseparable dependencies. The 1-D interval field method can be easily extended to multiple dimensions by constructing the basis functions as a vector-valued function of 1-D basis functions. In the 2-D scenario, specifically, the formulation for the k-th basis function

can be expressed as

$$b_{i,j}^{k}(\mathbf{x}) = b_{i,k}(x_1) b_{j,k}(x_2), i = 1, \ldots, n_{x_1}, j = 1, \ldots, n_{x_2}, \tag{7}$$

where $b_{i,k}(x_1)$ represents the B-spline basis function in the x direction, $b_{j,k}(x_2)$ is the B-spline basis function of y direction. The B-spline basis functions of the three-dimensional interval field, which can be represented as

$$b_{i,j,l}^{k}(\mathbf{x}) = b_{i,k}(x_1) b_{j,k}(x_2) b_{l,k}(x_3), i = 1, \ldots, N_{x_1}; j = 1, \ldots, N_{x_2}; l = 1, \ldots, N_{x_3}, \tag{8}$$

where $b_{l,k}(x_3)$ represents the B-spline basis function in the z direction. The 2/3-D interval fields can be calculated based on Eq. 5 and the 2/3-D B-spline basis functions.

Interval fields with deterministic local values

This subsection aims to generate interval fields with deterministic local values, which can be used to consider geotechnical in situ test data when generating interval fields. The advantage of this method is that it reduces epistemic uncertainty by fully utilizing the available in situ test data. Meanwhile, the epistemic uncertainty disappears at these locations with deterministic values, which implies that all realizations of the interval field must be passed through these deterministic points. In an attempt to make the method more understandable, a straightforward instance of deterministic local values is presented (Feng et al. 2023). Consider a 1-D region where an interval field with a determined value is constructed. Taking into account the given local values (x_0, h_0), the equation of the interval field can be expressed as

$$\psi^{\mathrm{I}}(x_0) = c^I + r^I \sum_{i=1}^{n} b_{i,k}(x_0) \xi_i^{\mathrm{I}} = h_0. \tag{9}$$

According to this equation, it is possible to compute the deterministic part of the interval variable. For the k-th degree of B-spline basis functions, there are $k+1$ basis functions with values

determined by Eq. 9. These deterministic interval variables can be calculated by

$$\sum_{i=m}^{m+k} b_{i,k}\left(x_o\right) \xi_i^{\mathrm{I}}=\frac{1}{r^I}\left(h_0-c^I\right), \tag{10}$$

where m corresponds to the m-th knot associated with the local value. This equation can calculate interval variables for interval fields with a single local value. For interval fields with multiple local deterministic values, the least squares method is used to compute interval variables in the region of influence of the local values. Then, the interval fields with deterministic local values are generated using Eq. 5. Finally, an example of interval fields with a deterministic local value is used to demonstrate the method. Fig. 2 depicts 50 samples of interval fields with a single deterministic local value. The parameters for this interval field are identical to the example in the preceding section, except for the inclusion of a local value.

PROPOSED FRAMEWORK

This paper proposes a framework for quantifying uncertainty in geotechnical engineering using the interval field method, building on the uncertainty quantification presented in our previous work. It not only tackles uncertainties concerning stratigraphic and spatial properties but also integrates in situ testing data into the interval field description. This framework is primarily based on the B-spline basis function-based interval field and is divided into three main sections. First, section 3.1 introduces the modeling of interval fields. In this part, the uncertainty of the stratigraphy is mainly considered and modeled by the B-spline basis function-based interval field. Then, the spatial uncertainty of geotechnical parameters is considered in each partition and modeled by the B-spline basis function-based interval field. Section 3.2 describes the implementation procedure of the finite element strength reduction method. In this section, we account for uncertainty in the boundaries within the geometric modeling. Finally, Section 3.3 presents the propagation method of the interval field. In this paper, the Bayesian global optimization method is employed to obtain the upper and lower bounds of the response values. The overall framework is depicted in the flowchart shown in Fig. 3.

Implementation of B-spline basis function-based interval fields

The purpose of this subsection is to generate interval fields that take into account uncertainties in stratigraphic and spatial properties. First, the stratification of the geology is determined based on the test data. This case involves the utilization of one-dimensional interval fields with deterministic local values. Then the interval field considering the uncertainty of spatial parameters is established within the same stratification. This case uses two/three-dimensional interval fields with local values. Determining the uncertainty modeling of the boundary or spatial properties or coupling of both is essential. Therefore, it is necessary to determine the kind of uncertainty to be considered for engineering. The interval field is generated after determining the type of uncertainty in geotechnical engineering. So the implementation procedure of the B-spline basis function-based interval field is described below.

1. First, the interval center, interval radius, and degree of B-spline basis function k of the interval field are determined. It is particularly emphasized that the center of the interval may be a function that varies with position. The degree of the B-spline basis function is two generally, which provides sufficient flexibility for most real-live engineering cases. The determination of these parameters can be achieved through various methods, such as interval field identification and quantification techniques or by referencing existing cases. In this paper, we adopt existing parameters, as the cases under consideration provide specific data, making it suitable for direct utilization.
2. Determine the dependency length according to the test data according to (Faes and Moens 2017a). It can also be determined by tuning the gradients of the realizations of the interval field to those seen in the data. This corresponds to setting a specific correlation length in a random field when following a probabilistic approach (Chen et al. 2020). In this study, the parameter of dependency length is sourced from the engineering literature.
3. Determining the knot span based on the dependency length from the preceding step is the focus here. To be specific, the knot span is calculated by Eq. 6.
4. Extend over the left and right sides of the domain to ensure that the B-spline basis functions

are defined over all geometric regions.

5. Discretise the domain and form all the knots into a knot vector. The knots' distance is determined by the span of the knots identified in step three.
6. A collection of k-th B-spline basis functions is generated through Eqs. 2 and 3.
7. Generating n-dimensional interval variables (n is determined by knot vector). The dimensionality varies according to the particular model being generated. In this context, the uncertainty of stratigraphic boundaries is a one-dimensional interval field, while the uncertainty of spatial properties is a two-dimensional interval field. It's important to note that the range of interval variables in this framework falls within [-1, 1].
8. Finally, the interval field is generated based on Eq. 5.

The implementation process for engineering problems with stratigraphic boundary uncertainty or spatial property uncertainty is achieved by the interval field method. The case of coupling the two requires more detailed descriptions. Firstly, the boundaries of different kinds of materials in geotechnical engineering are generated according to the method of the B-spline basis function-based interval field. As a result, each partition exhibits distinct material characteristics. Following the material boundary generation, we proceed to create B-spline basis function-based interval fields with spatial uncertainty independently within each subzone.

Finite element strength reduction method

This subsection provides a detailed explanation of computing the f_{s} using the finite element strength reduction method. Firstly, geometric modeling is introduced. Then the material parameters, boundary information and initial conditions of the model are introduced. Finally, the specific implementation steps of the strength reduction method are introduced.

A challenging problem for the geometric model is that the region's boundary after geological stratification is uncertain, generated by a one-dimensional interval field. For the numerical calculation problem of the uncertain region, a geometric transformation is used to solve this issue (Zheng et al. 2023). Specifically, the random domain $\Omega(\xi)$ is transformed into a reference domain $\overline{\Omega}(\xi)$,

and the mesh topology of the reference domain is used to represent the random domain. Thus, it is possible to avoid remeshing the random domain for each sample. The random coordinate $\mathbf{x}(\xi)$ is mapped into the deterministic coordinate $\overline{\mathbf{x}}$ according to

$$\overline{\mathbf{x}} = \Lambda^{-1}(\mathbf{x}(\xi), \xi), \tag{11}$$

where Λ^{-1} is inverse operator of the mapping operator. The random coordinates can be represented by deterministic coordinates as

$$\mathbf{x}(\xi) = \Lambda(\overline{\mathbf{x}}, \xi), \tag{12}$$

where Λ is the mapping operator. The modeling problem of the random domain can be solved according to the above transformation.

For the purpose of illustration in this paper, we adopt the Mohr-Coulomb model. The elastic modulus, Poisson's ratio and the material's weight are considered deterministic values. The cohesion and friction angle are considered interval parameters with spatial uncertainty. Lastly, the boundary conditions and initial conditions are applied to the numerical model.

Finally, the parameters of the interval field are input into the element of the numerical model of the slope, and the finite element strength reduction method is employed to compute the f_s of the slope (Cheng et al. 2007). In this approach, the reduced parameters encompass the cohesion and the friction angle. The numerical finite element analysis is implemented in this paper using OpenSees (Mazzoni 2006).

Bayesian global optimization

The Bayesian global optimization is an efficient optimization method based on a surrogate model, which is employed to determine the upper and lower boundaries of the f_s (Dang et al. 2022). The implementation process is briefly described below. The first step of the Bayesian global optimization algorithm involves selecting the initial sample points. In this stage, an initial set of samples is generated inside the interval using Latin hypercube sampling. Subsequently, the initial surrogate model is constructed using the initial samples and their corresponding function values. In

this stage, the Gaussian process regression method is used to develop the surrogate model. Finally, the genetic algorithm is used to find the maximum and minimum value of this surrogate model. For more details on Gaussian process regression, please refer to Williams and Rasmussen (2006). The initial Gaussian process regression $\mathcal{N}_0[\hat{\gamma}_0(\boldsymbol{\zeta}), s_0(\boldsymbol{\zeta})]$ serves as a surrogate model, where $\mathcal{N}_0[\cdot,\cdot]$ represents a normal distribution, and $\hat{\gamma}_0(\boldsymbol{\zeta})$ and $s_0(\boldsymbol{\zeta})$ are the mean value and the standard value of the predictive model, respectively.

The first step of Bayesian global optimization is to develop a surrogate model. The surrogate model generated from the initial points is in error, so it is very important to increase the number of sample points to improve the accuracy of the surrogate model. After increasing the number of sample points, the surrogate model can be denoted as $\mathcal{N}[\hat{\gamma}(\boldsymbol{\zeta}), s(\boldsymbol{\zeta})]$. From the results of the Gaussian process regression, an acquisition function is constructed to measure whether another point needs to be added, and the extreme value of the acquisition function is solved to determine the next sampling point. In the context of the minimization problem, the improvement of the objective function, denoted as $\theta(\boldsymbol{\zeta})$, is defined as

$$\theta(\boldsymbol{\zeta}) = \max\{\gamma_{\min} - \hat{\gamma}(\boldsymbol{\zeta}), 0\}, \tag{13}$$

where $\gamma_{\min}$ represents the current optimal objective function value, and $\hat{\gamma}(\boldsymbol{\zeta})$ is the set of parameters following a normal distribution. The expected value of $\theta(\boldsymbol{\zeta})$ is determined by Jones et al. (1998)

$$\mathbb{E}[\theta(\boldsymbol{\zeta})] = \begin{cases} (\gamma_{\min} - \hat{\gamma}(\boldsymbol{\zeta}))\Phi\left(\frac{\gamma_{\min} - \hat{\gamma}(\boldsymbol{\zeta})}{s(\boldsymbol{\zeta})}\right) + s(\boldsymbol{\zeta})\phi\left(\frac{\gamma_{\min} - \hat{\gamma}(\boldsymbol{\zeta})}{s(\boldsymbol{\zeta})}\right), s > 0 \\ 0, s = 0, \end{cases} \tag{14}$$

where $\mathbb{E}[\cdot]$ denotes the expectation operator, Φ is the standard normal cumulative distribution function, ϕ is the standard normal distribution probability density function, and $\hat{\gamma}(\boldsymbol{\zeta})$ and $s(\boldsymbol{\zeta})$ are the mean and standard deviation of the normal distribution of the Gaussian process regression model predictions, respectively.

Increasing the number of sample points until the accuracy of the surrogate model satisfies

the requirement, which can be judged according to the convergence criterion. The convergence criterion in this paper is defined as

$$\frac{|\max \mathbb{E}[\theta(\boldsymbol{\zeta})]|}{|\gamma_{\min}| + \delta} \leq \epsilon, \tag{15}$$

where $\max \mathbb{E}[\theta(\boldsymbol{\zeta})]$ denotes the maximum value of $\mathbb{E}[\theta(\boldsymbol{\zeta})]$, $\gamma_{\min}$ represents the minimum observed value of γ, δ is an infinitesimal value, ϵ is the threshold value. In this scenario, δ is set to 1e-6, and ϵ is set to 0.001. After the surrogate model satisfies the convergence criterion, the response values of all samples are recorded. The maximum and minimum of these values are the boundary values of the interval. This also means that the upper and lower bounds of the f_s of geotechnical engineering are obtained.

CASE STUDIES

This section demonstrates three examples to illustrate the efficiency of the proposed framework. The first case considers the modeling of an interval field of a slope with spatial uncertainty. The second case considers the interval field of a dyke with uncertainties in stratigraphy and spatial properties. Finally, the case of a three-dimensional dyke is considered. It should be noted that the cases selected in this paper only consider some idealized stratigraphy and further research is needed for more complex cases.

The case of considering spatial uncertainty

To evaluate the validity of the interval field for analyzing the stability of the slope, an assessment was performed using data obtained from an actual site situated in Shiraz, Iran (Johari and Fooladi 2020). The slope with 26 meters height and 30.96 degrees inclination was investigated. Fifteen boreholes were drilled at the surface to examine subsurface and soil properties. Fig. 4 illustrates the locations of the boreholes utilized in this case, along with cross-sectional views of the slopes. For this study, only two borehole test data from the same cross-section were utilized.

Firstly, the numerical model for this slope is developed, as shown in Fig. 4, in which the red edges represent the complete fixation, while the green edges denote only fixation in the horizontal

direction. The meshes of FEM in this paper are set as structured meshes to ensure that the number of meshes is deterministic while the geometry is changed. And the interval field meshes are set to be consistent with the meshes in FEM. The solver can be used in the principles of elastic viscoplastic soil behavior. In this specific case, the slope's cohesion and friction angle are treated as interval parameters, while the unit weight, Poisson's ratio, and modulus of elasticity are regarded as deterministic parameters. Specifically, the unit weight is 17.38 kN/m^3, the elastic modulus is 35,000 kN/m^2 and the Poisson's ratio is 0.3. Table 1 lists the parameters of the interval field.

First, the B-spline basis function-based interval field method is employed to generate a 2-D interval field within the specified region. Cohesion and friction angle intervals are determined using parameters obtained from in situ test data. The cohesion is set within the interval [5, 25] kPa and the friction angle interval is established as [18, 38] based on experimental data. It is important to note that interval boundaries are obtained from in situ test data (Imholz et al. 2020; Faes and Moens 2017a). The interval field in this study has horizontal and vertical dependence lengths denoted as l_h and l_v, respectively, with values set at 8.0 m and 4.0 m, as detailed in Johari and Fooladi (2020). It should be noted that the $\mathfrak{C}$-vine method is required if the cross-correlation between the interval fields of cohesion and friction angle needs to be considered (Faes and Moens 2020a). Known parameters from six locations in two cone penetration tests (CPT) boreholes are incorporated in the interval field. Figs. 5 and 6 present the generated interval fields of cohesion and friction angle, respectively. In these figures, the red circle represents this position has a deterministic value, which means that the samples of these interval fields have the same value in this position.

Subsequently, the finite element strength reduction method is applied to determine the f_{s} for the slope. Ultimately, the Bayesian global optimization method is utilized to obtain the interval of f_{s} for this slope. In this specific case, the resulting interval for f_{s} is [1.38, 2.14]. The depiction of the interval field results can be observed in Fig. 7. This figure also includes results for interval fields without considering in situ test data and results for conditional random field analyses. First, the effect of local values on the results of the interval field analysis is analyzed. As Fig. 7 shows, the result of the interval field without considering local values is [1.22, 2.22]. It can be seen that

integrating in situ test data to reduce the epistemic in the interval field definition also reduces the epistemic uncertainty in the response. The interval of the f_s of geotechnical engineering will be gradually reduced when enough data are measured. The effect of the f_s interval is relatively minor due to the fewer local values of the geotechnical engineering in this case. This underscores the significance of in situ test data in the uncertainty analysis of geotechnical engineering.

Then, comparing the interval field method with the conditional random field (Johari and Fooladi 2020) using in situ test data demonstrates that the interval field method encompasses all the data from the random field, which implies that the interval field method provides more comprehensive information. This is because the parameters of the interval field have a relatively wide range. If sparse data are used to obtain smaller intervals, it may lead to high risk. For geotechnical engineering with extensive datasets, the random field method may be an option because of the parameter distributions and spatial uncertainties that can be obtained by statistical methods, which makes the obtained results more accurate because it can represent the statistical properties of the parameters. However, it is difficult to obtain the parameters of the random field for sparse data, so the random field method requires some assumptions for this case. It may produce misleading conclusions and might provide overconfidence due to insufficient conservativeness. Therefore it should be careful when using the random field method for sparse data cases.

In contrast, the interval field method, by focusing on extreme values without considering their probability of occurrence, assumes a worst-case scenario, ensuring safety when dealing with uncertainty. This conservative approach is crucial in engineering decisions, providing safeguards for worst-case situations and making it suitable for scenarios requiring high safety and conservatism. Thus, the interval field method is valuable for risk assessments involving low-probability but high-consequence events, such as extreme geohazard events. Moreover, the interval method does not require detailed probability distribution information, making it especially useful when data is limited. For instance, in newly developed geological areas where detailed soil testing data may not be available, engineers can use the interval method based on existing experience and limited data to estimate ranges of soil parameters for uncertainty propagation. Additionally, the

interval method is more efficient than stochastic methods like Monte Carlo simulations because it only evaluates extreme combinations of parameters without needing extensive random sampling. Overall, the interval method, by emphasizing worst-case scenarios and reducing dependence on detailed probability information, provides a safe, reliable, and efficient analysis tool in engineering, particularly suited for situations with sparse data and high uncertainty. It should be noted that both the random field and interval field methods discussed here consider only epistemic uncertainty.

This case study demonstrates the effectiveness of the interval fields in addressing spatial uncertainty for slopes in geotechnical engineering, particularly when data is scarce. Then, we emphasize the importance of in situ test data for uncertainty analysis in geotechnical engineering. The method can be applied with or without such data, depending on project specifics. In geotechnical engineering, the interval field method is particularly useful when in situ test data is unavailable. However, for projects with limited data, incorporating local values can further enhance the analysis. Finally, a comparison of the interval field method proposed with the established random field method is presented in detail, demonstrating the range of applicability and advantages of the proposed method. In engineering applications with critical consequences, the interval field method is particularly valuable for engineering projects with sparse data, as it emphasizes the critical role of extreme values in decision-making.

The case of considering uncertainty in stratigraphic and spatial properties

The second scenario involves a real dyke. The "Leendert de Boerspolder" is a small polder in South Holland, situated to the south of one of the economically significant polders in the Netherlands. de Gast et al. (2021) conducted detailed testing of the dyke. Fig. 8 illustrates a top view of the dyke. The cross-section of the dyke, selected for this case is highlighted within the blue circle in this figure. And Fig. 9 depicts the geometric model, which has a length and height of approximately 28m and 10m, respectively. The purple line indicates the positions of CPT boreholes, revealing that this cross-section includes three CPT boreholes. It is divided into four layers: dyke material, peat, organic clay, and silty clay. The obtained test parameters must be

converted into undrained shear strength (s_u) for subsequent analysis, which can be expressed as

$$s_u = \frac{q_t - \sigma_v}{N_{kt}} \tag{16}$$

where q_t represents the total cone resistance, σ_v denotes the total vertical stress, and N_{kt} is an empirical correction factor with a range of 10 to 20. The assigned values of N_{kt} for the four soil layers are as follows: dyke material, N_{kt}=20; peat, N_{kt}=15; organic clay, N_{kt}=10; and silty clay, N_{kt}=10. Table 2 presents the parameters of the interval field for this dyke engineering. The Mohr-Coulomb criterion is utilized as the material constitutive model, and the finite element strength reduction method is applied to compute the f_{s} for the dyke, with the s_u serving as the reduced parameter.

Then the interval field for the parameter of s_u of the dyke is generated. The meshes in the numerical model were set to structured meshes and checked for the accuracy of their calculations. When generating the interval field, the interval field meshes are set to the meshes of FEM for this dyke. These are to ensure that the number of meshes is deterministic while the geometry is changed. The next step is to generate an interval field model of this dyke. The parameters required for constructing the interval field include the degree of B-spline basis functions, interval center and radius, and horizontal and vertical dependence length. It should be noted that determining horizontal and vertical dependency lengths from sparse data is challenging, but can be addressed through various approaches, such as leveraging the expertise and accumulated experience of engineers. For this scenario, the degree of B-spline basis function with the value of 2. The interval center and interval radius values are established based on the s_u parameters at the CPT test point. Specifically, attention is devoted to soils across various layers and the spatial uncertainty inherent within each layer. According to test data, the horizontal dependence length and vertical dependence length are determined through point estimation. Consequently, the strata exhibit distinct parameters from one another. The generation of the interval fields based on these parameters is illustrated in Fig. 10. The dyke case with spatial uncertainty after considering deterministic stratigraphy is analyzed. Finally,

the intervals of f_s for the dykes are computed according to Bayesian global optimization methods. For this dyke, the calculated interval for f_s is [0.80, 1.08].

Then the uncertainty of coupling stratigraphic and spatial properties is analyzed. In this context, we categorize the geological strata into four layers based on distinct geotechnical materials, resulting in three stratigraphic boundaries. To represent uncertainty, we employ one-dimensional interval fields for each of these boundaries. For each geotechnical material within a stratum, a two-dimensional interval field is used to represent the uncertainty of the geotechnical spatial properties. Detailed insights into this methodology are provided in Section 3, where we comprehensively expound on the specific aspects and nuances of our approach.

The initial stage of uncertainty analysis in geotechnical engineering involves the creation of an interval field that accounts for the uncertainties related to stratigraphic and spatial properties. In this step, it is necessary to determine the parameters of the one-dimensional interval field of the stratigraphic boundary first. The interval mean values of the interval fields for the stratigraphic boundaries of organic clay and silt clay are set to the already estimated stratigraphic boundary, the interval radius is set to 0.1, and the spatial dependence length is set to 5. The interval mean of the interval field of the stratigraphic boundary of the silty clay and peat is set to the already estimated stratigraphic boundary, the interval radius is set to 0.1, and the spatial dependence length is set to 5. The interval mean of the interval field of the stratigraphic boundary of peat and dyke material is set to the already estimated stratigraphic boundary, the interval radius is set to 0.1, and the spatial dependence length is set to 3. The one-dimensional interval fields are generated separately according to the interval field parameters of the determined stratigraphic boundaries. Then the two-dimensional interval field parameters of geotechnical spatial properties within each stratum are determined separately. Table 2 shows the parameters of its interval field. The geometric boundary of each stratum is changed due to the uncertainty of the stratum boundary. Therefore, a geometric transformation method is used in this paper to solve this problem, the details of which are shown in Section 3.2. The interval fields are generated separately within each stratum according to the determined interval field parameters. Finally, by combining the interval fields generated

for stratigraphic boundaries and spatial properties within the stratum, we obtain interval fields that account for the uncertainties in both stratigraphic and spatial properties. The second stage in assessing the uncertainty of geotechnical engineering involves determining the f_s through the utilization of interval fields generated via the finite element strength reduction method. To execute this step, OpenSees is employed for finite element analysis, and comprehensive implementation instructions can be found in Section 3.2. Subsequently, the third step in analyzing the uncertainty of coupling stratigraphic and spatial properties in geotechnical engineering is to calculate the interval boundaries of the f_s of geotechnical engineering using the Bayesian optimization method. Specific details and parameter settings for this optimization technique are elaborated in Section 3.3.

The interval of the f_s obtained from the analysis using the interval field method for this case is [0.78, 0.98]. Then two samples are shown corresponding to the maximum and minimum values of f_s respectively, as presented in Fig. 11 and Fig. 12. In these figures, the bold black line represents the stratum's boundary, while the red circles indicate locations with determinate values. Fig. 11 (a) and Fig. 12 (a) show the uncertainty of the stratigraphy. Fig. 11 (b) and Fig. 12 (b) show the spatial property uncertainty within the strata. It can be noticed that the strata boundary corresponding to the maximum value of f_s varies more significantly. Compared to scenarios where stratigraphic uncertainty is not considered, the f_s range is significantly narrower, and the minimum value of the f_s is reduced. This indicates that accounting for stratigraphic uncertainty increases the risk in geotechnical engineering. In this specific case, the impact is mitigated because the variability of stratigraphic boundaries considered is small. For real situations, its variability may be higher. So it's important to note that the uncertainty in stratigraphic boundaries may have a substantial influence on the f_s values in geotechnical engineering. Therefore, it is crucial to consider the uncertainty of the coupled stratigraphic and spatial properties for critical engineering.

The case of three-dimensional dyke

The effectiveness of this method in the context of three-dimensional engineering is illustrated in this subsection. The example employed here corresponds to case 2, so the cross-section of the geometric model is shown in Fig. 9, and the parameters are referred to in Table 2. The three-

dimensional model was generated by stretching the dyke of case 2 by 10 meters. The geotechnical parameters and stratigraphic boundaries are consistent with case 2. The uncertainty of coupling stratigraphic boundaries and spatial properties of this three-dimensional dyke is considered in this case. The interval fields of the dyke model were generated with three directions of parameters due to the three-dimensional model. The interval field parameters for the cross-section of this dyke model are the same as in case 2. The interval field parameters for the stretched direction of the model were determined based on the in situ test data. The three-dimensional interval field was generated and analyzed for its safety based on the parameters of this dyke numerical model.

The uncertainty analysis of this three-dimensional dyke by the interval field method has three main steps. The initial step involves creating an interval field model for the geotechnical parameters of this 3-D dyke. First, the uncertainty of the dyke's stratigraphy is generated as an interval field. In this step, it is assumed that the three-dimensional dyke has consistent stratigraphic boundaries. Then, the interval fields of the spatial properties of the geotechnical parameters are generated within the same stratum. In this step, the spatial dependence length of this three-dimensional interval field in the stretching direction is set to 5, and the rest of the parameters are the same as in case 2. The interval field for the s_u of this three-dimensional dyke is obtained by combining the generated interval fields above. Fig. 13 shows the interval field of s_u generated by the geotechnical parameters of this three-dimensional dyke. The second step is calculating the f_{s} of the dyke using the finite element strength reduction method. The last step is to calculate the interval of the f_{s} of this dyke using the Bayesian optimization method.

The interval of the f_{s} obtained from the analysis using the interval field method for the three-dimensional dyke is [0.78, 1.08]. It has the same lower bound of f_{s}, while its upper bound is larger than the two-dimensional case. The three-dimensional analysis obtains a larger interval of f_{s} than the two-dimensional dyke analysis. The conclusions obtained from the available literature indicate that the two-dimensional analysis of geotechnical engineering obtains more conservative results (Griffiths and Marquez 2007). However, in this paper, the lower bound of the f_{s} is the same as that of the two-dimensional geotechnical engineering, probably due to the effect of three-

dimensional spatial uncertainty is considered. Therefore, it is necessary to perform a complete analysis of important geotechnical engineering because the spatial variability in three dimensions has the potential to have a very negative impact on this engineering.

CONCLUSIONS

This paper proposes a framework for the interval field-based method designed to address uncertainty in the stratigraphic and spatial properties of geotechnical engineering. It is particularly suitable for situations with sparse data while also allowing for the integration of in situ test data into the interval field representation. The first step involves generating an interval field using the B-spline basis function-based interval field method. This process takes into account the uncertainties in coupling with stratigraphic and spatial properties in geotechnical engineering, while sparse data with deterministic values at specific locations are also considered. Subsequently, the finite element strength reduction method is employed to compute the f_s for geotechnical engineering. Ultimately, the Bayesian global optimization method is employed to ascertain the interval boundaries of the f_s. The key conclusions drawn from this study include the following:

1. In geotechnical engineering, the interval boundaries are directly determined from the test data, eliminating the necessity for any statistical assumptions. This makes the interval field method particularly suitable for projects with low failure probabilities but significant consequences. It efficiently leverages sparse test data to provide thorough analyses, yielding conservative results that are highly useful during the pre-design phase of critical projects with limited data.
2. In-situ test data play a crucial role in reducing uncertainty. As the quantity of such data increases, the range of outcomes determined by the interval field method narrows, improving result accuracy.
3. Moreover, the uncertainty related to stratigraphic boundaries has a substantial impact on geotechnical engineering results. Therefore, considering the uncertainty of spatial properties in combination with geotechnical stratigraphy uncertainty is essential to improving the

reliability of the analytical results.

While the present study has yielded promising results, there is a need for additional research. In future investigations, it is anticipated that more types of uncertainties and complex models can be adapted into the proposed framework.

DATA AVAILABILITY STATEMENT

Some or all data, models, or code that support the findings of this study are available from the corresponding author upon reasonable request.

ACKNOWLEDGMENTS

The first author is supported by the China Scholarship Council (CSC No. 202108420064). Matthias Faes gratefully acknowledges funding from the German Research Foundation (DFG) under grant nr. 530326817.

REFERENCES

Beer, M., Zhang, Y., Quek, S. T., and Phoon, K. K. (2013). "Reliability analysis with scarce information: Comparing alternative approaches in a geotechnical engineering context." *Structural Safety*, 41, 1–10.

Callens, R. R., Faes, M. G., and Moens, D. (2021). "Local explicit interval fields for non-stationary uncertainty modelling in finite element models." *Computer Methods in Applied Mechanics and Engineering*, 379, 113735.

Cami, B., Javankhoshdel, S., Phoon, K.-K., and Ching, J. (2020). "Scale of fluctuation for spatially varying soils: estimation methods and values." *ASCE-ASME Journal of Risk and Uncertainty in Engineering Systems, Part A: Civil Engineering*, 6(4), 03120002.

Chen, Z.-Y., Imholz, M., Li, L., Faes, M., and Moens, D. (2020). "Transient landing dynamics analysis for a lunar lander with random and interval fields." *Applied Mathematical Modelling*, 88, 827–851.

Cheng, Y. M., Lansivaara, T., and Wei, W. (2007). "Two-dimensional slope stability analysis by limit equilibrium and strength reduction methods." *Computers and geotechnics*, 34(3), 137–150.

Chwała, M., Phoon, K.-K., Uzielli, M., Zhang, J., Zhang, L., and Ching, J. (2022). "Time capsule for geotechnical risk and reliability." *Georisk: Assessment and Management of Risk for Engineered Systems and Geohazards*, 1–28.

Cox, M. G. (1972). "The numerical evaluation of b-splines." *IMA Journal of Applied mathematics*, 10(2), 134–149.

Dang, C., Wei, P., Faes, M. G., Valdebenito, M. A., and Beer, M. (2022). "Interval uncertainty propagation by a parallel bayesian global optimization method." *Applied Mathematical Modelling*, 108, 220–235.

de Gast, T., Hicks, M. A., Van den Eijnden, A. P., and Vardon, P. J. (2021). "On the reliability assessment of a controlled dyke failure." *Géotechnique*, 71(11), 1028–1043.

Der Kiureghian, A. and Ditlevsen, O. (2009). "Aleatory or epistemic? does it matter?." *Structural safety*, 31(2), 105–112.

Ellingwood, B., Maes, M., Michael Bartlett, F., Beck, A. T., Caprani, C., Der Kiureghian, A., Dueñas-Osorio, L., Galvão, N., Gilbert, R., Li, J., Matos, J., Mori, Y., Papaioannou, I., Parades, R., Straub, D., and Sudret, B. (2024). "Development of methods of structural reliability." *Structural Safety*, 102474.

Faes, M. and Moens, D. (2017a). "Identification and quantification of spatial interval uncertainty in numerical models." *Computers & Structures*, 192, 16–33.

Faes, M. and Moens, D. (2017b). "Quantification of non-homogeneous interval uncertainty based on scatter in modal properties." *Procedia engineering*, 199, 1216–1221.

Faes, M. and Moens, D. (2020a). "On auto-and cross-interdependence in interval field finite element analysis." *International Journal for Numerical Methods in Engineering*, 121(9), 2033–2050.

Faes, M. and Moens, D. (2020b). "Recent trends in the modeling and quantification of non-probabilistic uncertainty." *Archives of Computational Methods in Engineering*, 27, 633–671.

Feng, C., Broggi, M., Faes, M., and Beer, M. (2023). "Geotechnical uncertainty analysis with sparse data using interval field method." *14th International Conference on Applications of Statistics and Probability in Civil Engineering(ICASP14)*.

Feng, C., Faes, M., Broggi, M., Dang, C., Yang, J., Zheng, Z., and Beer, M. (2022). "Application of interval field method to the stability analysis of slopes in presence of uncertainties." *Computers and Geotechnics*, 105060.

Feng, C., Valdebenito, M. A., Chwała, M., Liao, K., Broggi, M., and Beer, M. (2024). "Efficient slope reliability analysis under soil spatial variability using maximum entropy distribution with fractional moments." *Journal of Rock Mechanics and Geotechnical Engineering*, 16(4), 1140–1152.

Gong, W., Zhao, C., Juang, C. H., Zhang, Y., Tang, H., and Lu, Y. (2021). "Coupled characterization of stratigraphic and geo-properties uncertainties–a conditional random field approach." *Engineering Geology*, 294, 106348.

Griffiths, D. and Marquez, R. (2007). "Three-dimensional slope stability analysis by elasto-plastic finite elements." *Geotechnique*, 57(6), 537–546.

Guo, X., Dias, D., and Pan, Q. (2019). "Probabilistic stability analysis of an embankment dam considering soil spatial variability." *Computers and Geotechnics*, 113, 103093.

Hu, H., Wu, Y., Batou, A., and Ouyang, H. (2022). "B-spline based interval field decomposition method." *Computers & Structures*, 272, 106874.

Imholz, M., Faes, M., Vandepitte, D., and Moens, D. (2020). "Robust uncertainty quantification in structural dynamics under scarse experimental modal data: A bayesian-interval approach." *Journal of Sound and Vibration*, 467, 114983.

Jiang, C., Han, X., Lu, G., Liu, J., Zhang, Z., and Bai, Y. (2011). "Correlation analysis of non-probabilistic convex model and corresponding structural reliability technique." *Computer Methods in Applied Mechanics and Engineering*, 200(33-36), 2528–2546.

Jiang, S.-H., Huang, J., Griffiths, D., and Deng, Z.-P. (2022). "Advances in reliability and risk analyses of slopes in spatially variable soils: a state-of-the-art review." *Computers and Geotechnics*, 141, 104498.

Johari, A. and Fooladi, H. (2020). "Comparative study of stochastic slope stability analysis based on conditional and unconditional random field." *Computers and Geotechnics*, 125, 103707.

667 Jones, D. R., Schonlau, M., and Welch, W. J. (1998). "Efficient global optimization of expensive
668 black-box functions." *Journal of Global optimization*, 13(4), 455.
669 Juang, C. H., Zhang, J., Shen, M., and Hu, J. (2019). "Probabilistic methods for unified treatment
670 of geotechnical and geological uncertainties in a geotechnical analysis." *Engineering geology*,
671 249, 148–161.
672 Liu, L.-L. and Wang, Y. (2022). "Quantification of stratigraphic boundary uncertainty from limited
673 boreholes and its effect on slope stability analysis." *Engineering Geology*, 306, 106770.
674 Mazzoni, S. (2006). "Opensees command language manual." *Pacific Earthquake Engineering*
675 *Research (PEER) Center*, 264(1), 137–158.
676 McMillan, H., Jackson, B., Clark, M., Kavetski, D., and Woods, R. (2011). "Rainfall uncertainty in
677 hydrological modelling: An evaluation of multiplicative error models." *Journal of Hydrology*,
678 400(1-2), 83–94.
679 Moens, D., De Munck, M., Desmet, W., and Vandepitte, D. (2011). "Numerical dynamic analysis
680 of uncertain mechanical structures based on interval fields." *IUTAM Symposium on the Vibration*
681 *Analysis of Structures with Uncertainties: Proceedings of the IUTAM Symposium on the Vibra-*
682 *tion Analysis of Structures with Uncertainties held in St. Petersburg, Russia, July 5–9, 2009*,
683 Springer, 71–83.
684 Montoya-Noguera, S., Zhao, T., Hu, Y., Wang, Y., and Phoon, K.-K. (2019). "Simulation of non-
685 stationary non-gaussian random fields from sparse measurements using bayesian compressive
686 sampling and karhunen-loève expansion." *Structural Safety*, 79, 66–79.
687 Phoon, K.-K. (2023). "What geotechnical engineers want to know about reliability." *ASCE-ASME*
688 *Journal of Risk and Uncertainty in Engineering Systems, Part A: Civil Engineering*, 9(2),
689 03123001.
690 Phoon, K.-K. and Ching, J. (2018). *Risk and reliability in geotechnical engineering*. CRC Press.
691 Phoon, K.-K. and Kulhawy, F. H. (1999). "Characterization of geotechnical variability." *Canadian*
692 *geotechnical journal*, 36(4), 612–624.
693 Piegl, L. and Tiller, W. (1996). *The NURBS book*. Springer Science & Business Media.

Sofi, A. (2015). "Structural response variability under spatially dependent uncertainty: Stochastic versus interval model." *Probabilistic Engineering Mechanics*, 42, 78–86.

Sudret, B. and Der Kiureghian, A. (2000). *Stochastic finite element methods and reliability: a state-of-the-art report*. Department of Civil and Environmental Engineering, University of California.

Uribe, F., Papaioannou, I., Betz, W., and Straub, D. (2020). "Bayesian inference of random fields represented with the karhunen–loève expansion." *Computer Methods in Applied Mechanics and Engineering*, 358, 112632.

van Mierlo, C., Faes, M. G., and Moens, D. (2021). "Inhomogeneous interval fields based on scaled inverse distance weighting interpolation." *Computer Methods in Applied Mechanics and Engineering*, 373, 113542.

Wang, L., Wu, C., Tang, L., Zhang, W., Lacasse, S., Liu, H., and Gao, L. (2020). "Efficient reliability analysis of earth dam slope stability using extreme gradient boosting method." *Acta Geotechnica*, 15, 3135–3150.

Wang, Y., Zhao, T., and Phoon, K.-K. (2018). "Direct simulation of random field samples from sparsely measured geotechnical data with consideration of uncertainty in interpretation." *Canadian Geotechnical Journal*, 55(6), 862–880.

Wang, Z., Zhang, J., and Huang, H. (2023). "Interpreting random fields through the u-net architecture for failure mechanism and deformation predictions of geosystems." *Geoscience Frontiers*, 101720.

Williams, C. K. and Rasmussen, C. E. (2006). *Gaussian processes for machine learning*, Vol. 2. MIT press Cambridge, MA.

Xiao, L., Huang, H., and Zhang, J. (2017). "Effect of soil spatial variability on ground settlement induced by shield tunnelling." *Geo-Risk 2017*, 330–339.

Yan, W., Shen, P., Zhou, W.-H., and Ma, G. (2023). "A rigorous random field-based framework for 3d stratigraphic uncertainty modelling." *Engineering Geology*, 323, 107235.

Zhang, J.-Z., Liu, Z.-Q., Zhang, D.-M., Huang, H.-W., Phoon, K.-K., and Xue, Y.-D. (2022). "Improved coupled markov chain method for simulating geological uncertainty." *Engineering*

721 *Geology*, 298, 106539.

722 Zhao, C., Gong, W., Li, T., Juang, C. H., Tang, H., and Wang, H. (2021). "Probabilistic char-
723 acterization of subsurface stratigraphic configuration with modified random field approach."
724 *Engineering Geology*, 288, 106138.

725 Zhao, T., Hu, Y., and Wang, Y. (2018). "Statistical interpretation of spatially varying 2d geo-data
726 from sparse measurements using bayesian compressive sampling." *Engineering Geology*, 246,
727 162–175.

728 Zheng, Z., Valdebenito, M., Beer, M., and Nackenhorst, U. (2023). "A stochastic finite element
729 scheme for solving partial differential equations defined on random domains." *Computer Methods*
730 *in Applied Mechanics and Engineering*, 405, 115860.

List of Tables

TABLE 1. Material parameters for the slope in case 1

Soil parameters	Interval parameters	l_{h}	l_{v}
c (kPa)	[5, 25]	8	4
φ (°)	[18, 38]	8	4

TABLE 2. Material parameters of the dyke in case 2

Materials	E (kN/^{2})	λ	Interval of s_u	l_h	l_v
Dyke material	5600	0.3	[5, 25]	2.13	0.4
Peat	1700	0.3	[5, 15]	2.84	0.76
Organic clay	5200	0.35	[5, 20]	2.84	0.76
Silty clay	5300	0.35	[15, 25]	2.10	0.26

List of Figures

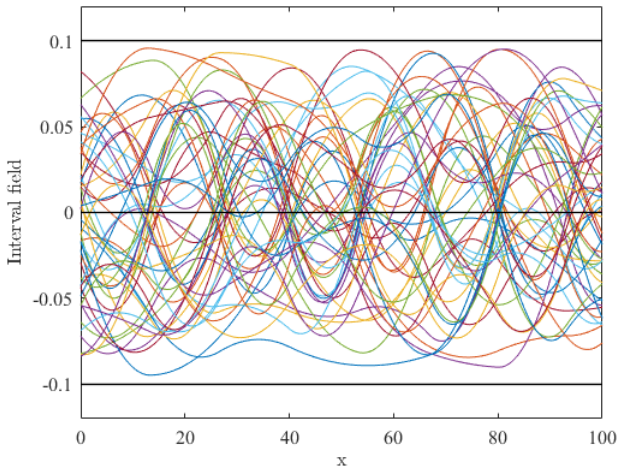

Fig. 1. Generation of 50 interval field realizations

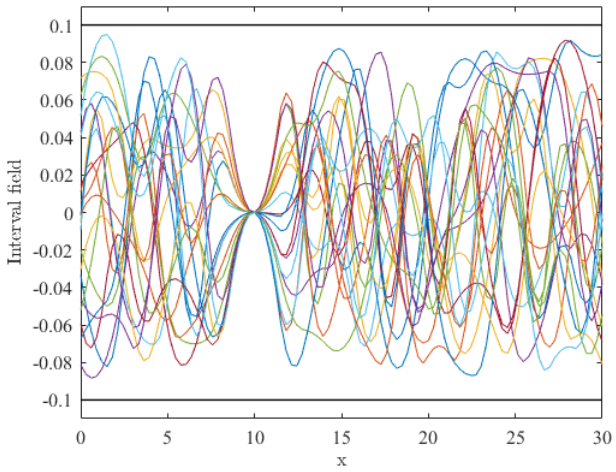

Fig. 2. Realizations of 50 interval field with one local value

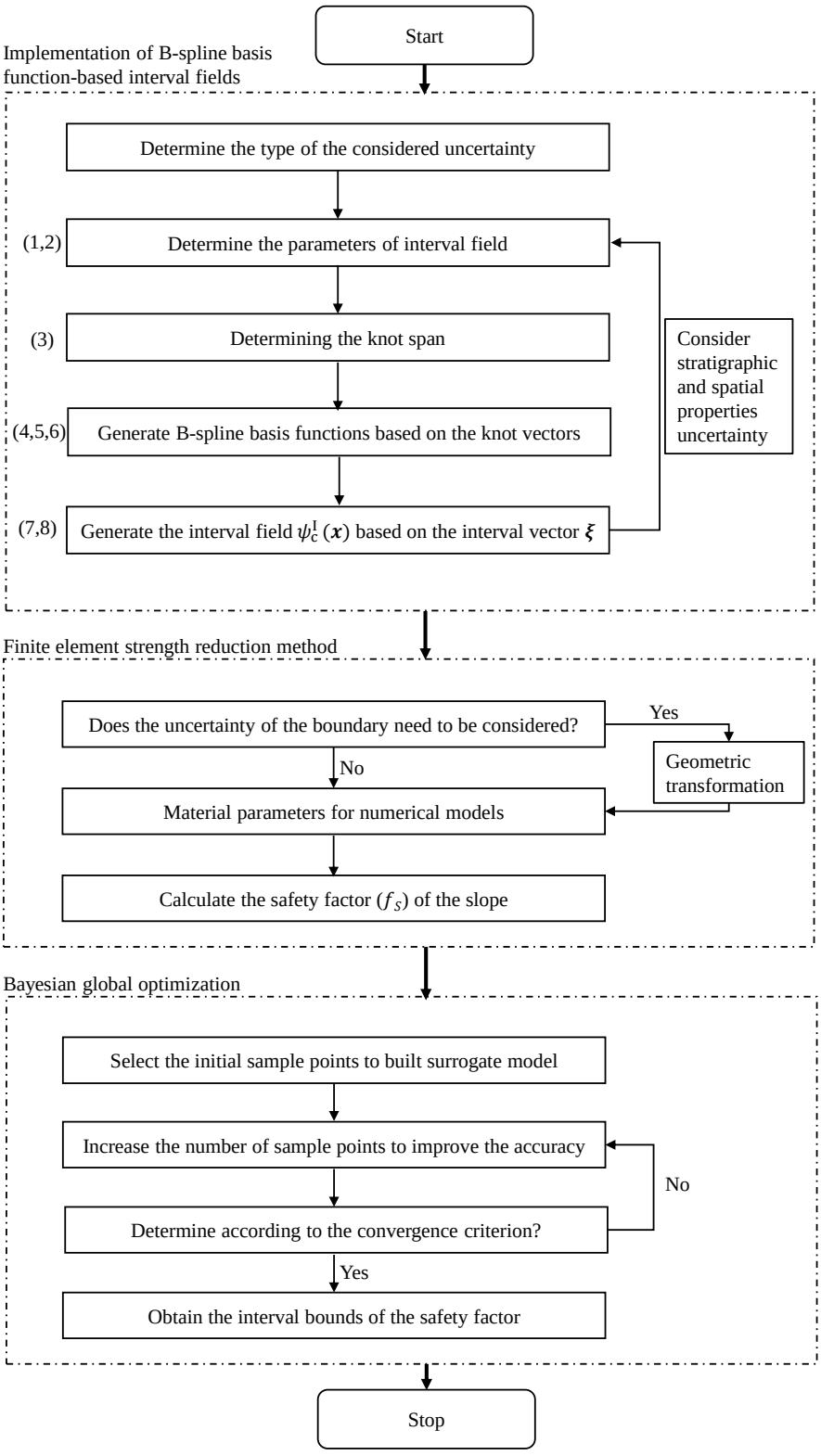

Fig. 3. Flowchart of the proposed framework

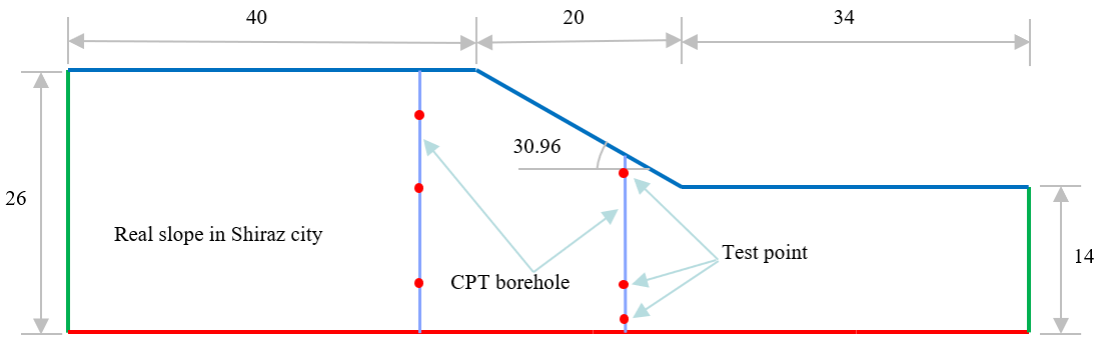

Fig. 4. Geometric model of the slope (Unit: m)

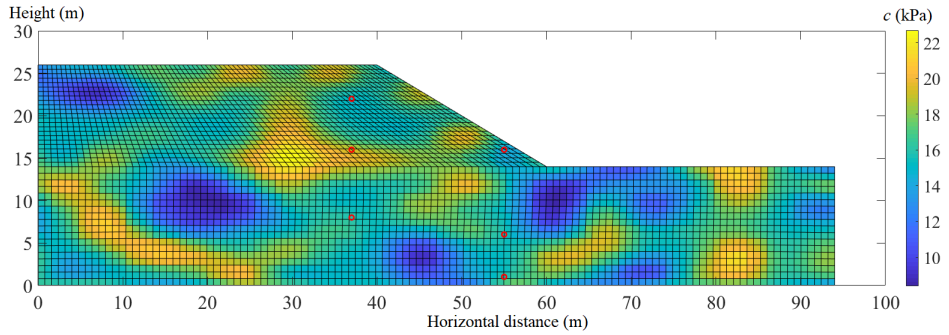

Fig. 5. A sample of the interval field of cohesion for the slope (kPa).

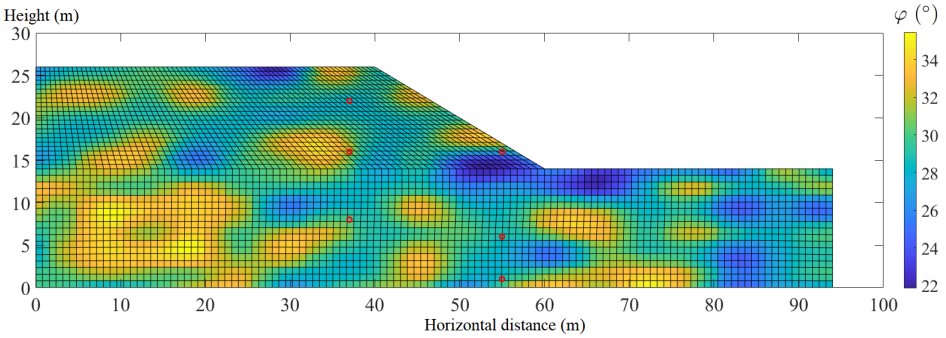

Fig. 6. A sample of the interval field of friction angle for the slope (°)

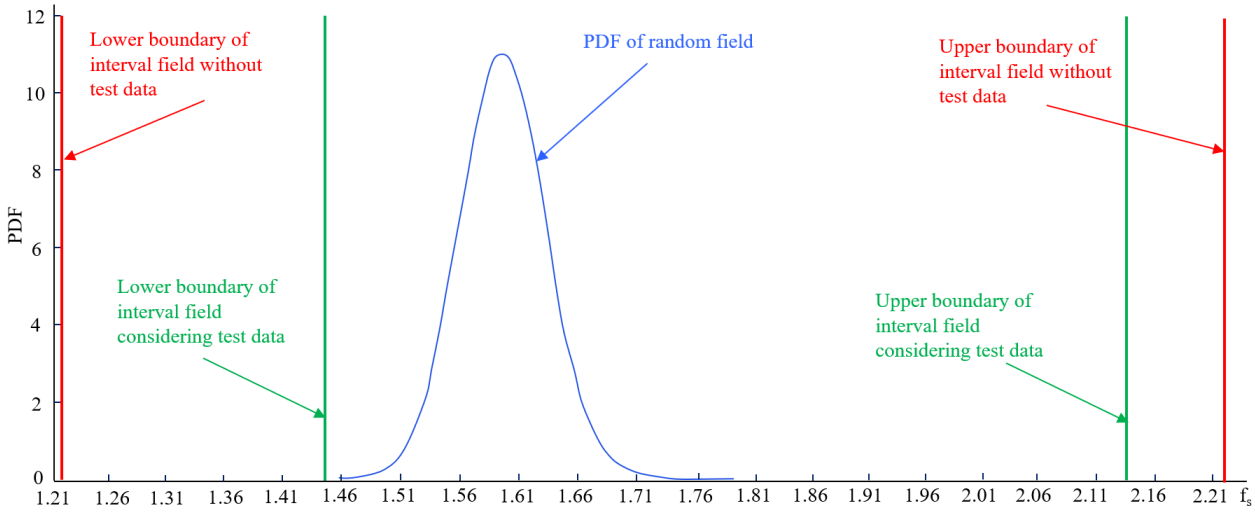

Fig. 7. Results of the interval field method (Includes results for interval fields without considering in situ test data and results for conditional random field analyses (Johari and Fooladi 2020))

Fig. 8. Top view of the dyke (modified from (de Gast et al. 2021))

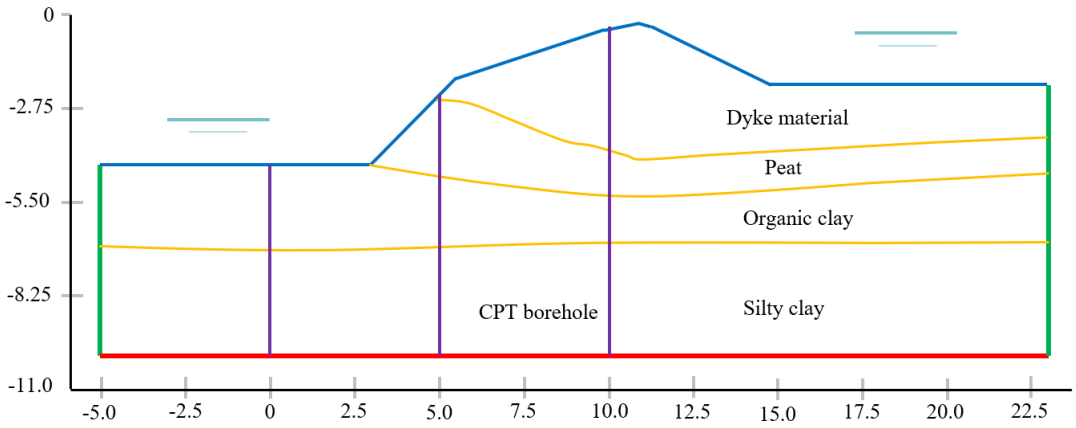

Fig. 9. Geometric modeling of the dyke (Unit: m)

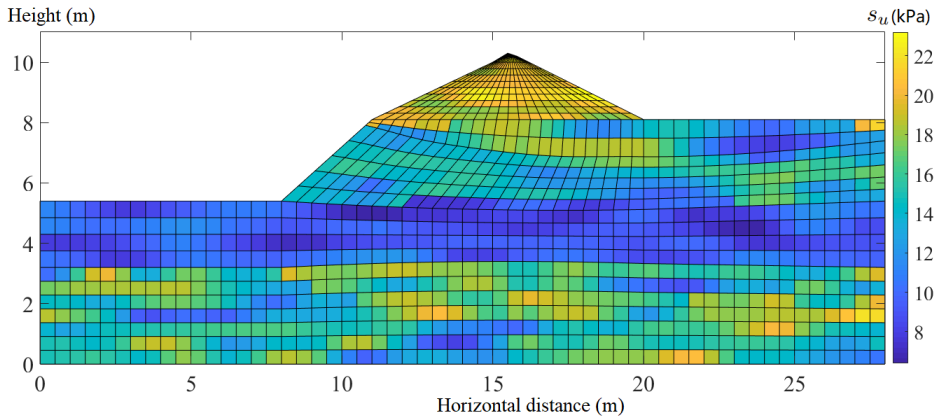

Fig. 10. Interval field realization of the s_u (kPa) without stratigraphic boundary uncertainty.

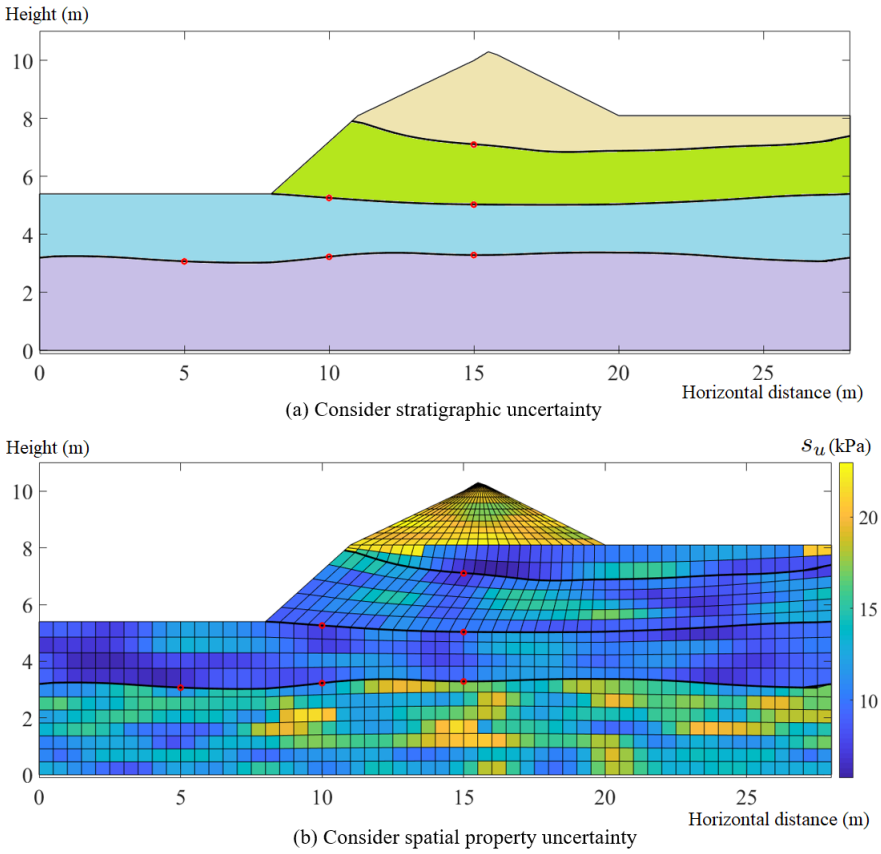

Fig. 11. Interval field realization of the s_u corresponds to the maximum of f_s: (a) Sample with stratigraphic uncertainty; (b) Sample with Coupling stratigraphic and spatial property uncertainty.

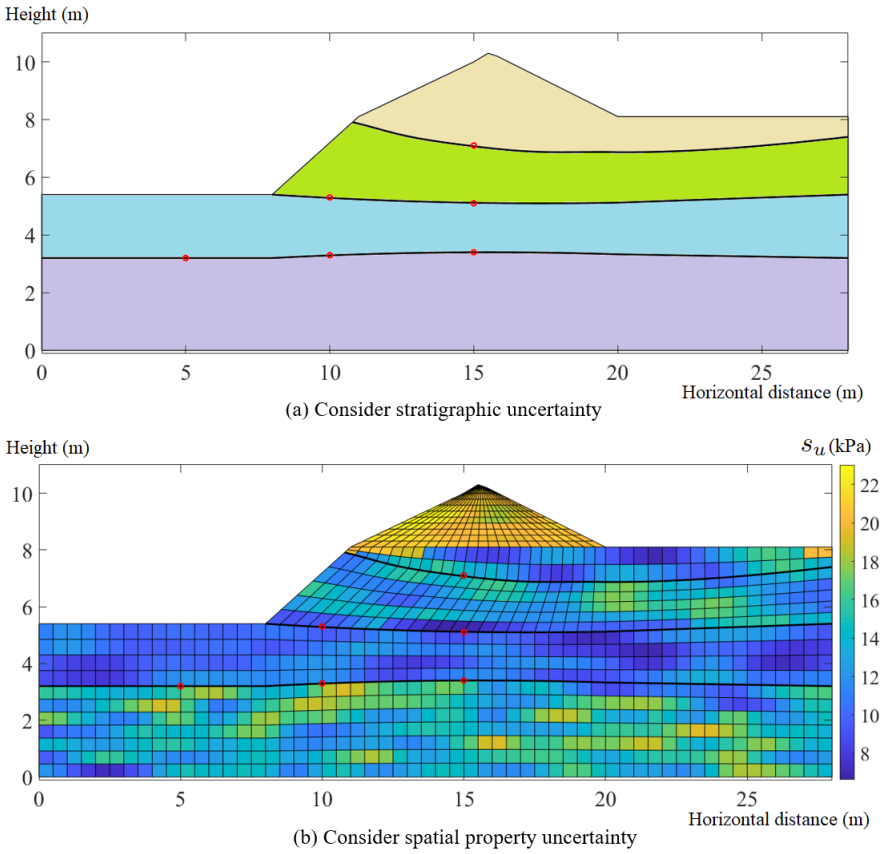

Fig. 12. Interval field realization of the s_u corresponds to the minimum of f_s: (a) Sample with stratigraphic uncertainty; (b) Sample with Coupling stratigraphic and spatial property uncertainty.

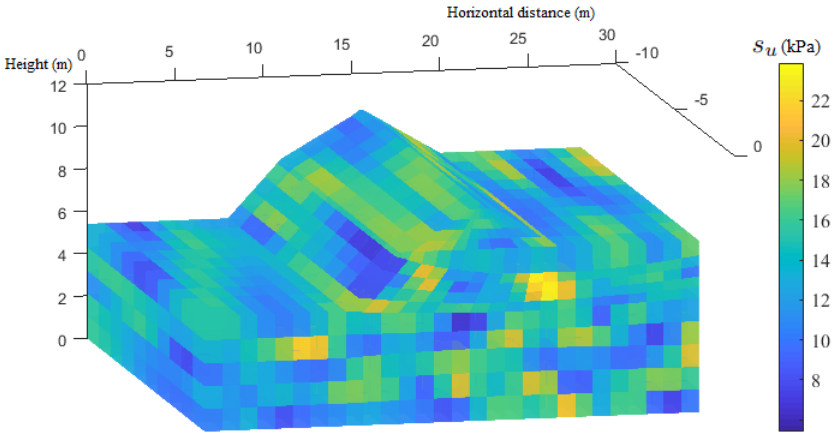

Fig. 13. Interval field realization of the s_u of three-dimensional dyke (kPa)